

Dynamic Behaviour of Flow through Multi-Stage Restricting Orifices

Abdulrazaq A. Araoye¹, Hasan M. Badr¹, Wael H. Ahmed²

¹Mechanical Engineering Department, King Fahd University of Petroleum & Minerals
Dhahran 31261, Saudi Arabia

g201306410@kfupm.edu.sa; badrhm@kfupm.edu.sa

²School of Engineering, University of Guelph, Guelph,
Ontario N1G 2W1, Canada

ahmedw@uoguelph.ca

Abstract - Orifices are widely used as flow restriction devices for the sake of pressure control, flowrate control or both. In these cases, the use of restricting orifices often result in high hydraulic losses, severe erosion in the presence of solid particles; cavitation in liquid flows, choking in gas flows in addition to noise and vibration. In this paper, the characteristics of flow through a multi-stage orifice plates fitted in a horizontal pipe of 25.4mm internal diameter has been investigated. Computational fluid dynamics calculations were performed using the realizable $k-\epsilon$ eddy viscosity model to predict the flow features. The effects of various parameters such as pipe flow velocity in the range 1–4m/s, orifice spacing of 1D and 2D, and orifice plate diameter ratios of 0.63 on axial velocity and pressure distributions were obtained. The location of vena contracta associated with the first orifice was found to be independent of addition of second orifice but varies with orifice diameter ratios while the presence of vena contracta downstream of the second orifice was found to depend on the orifice spacing. Not only the flow structure between the two orifices and downstream the second orifice was found to depend on the orifice spacing but also the total pressure drop and hydraulic losses. Orifice spacing of 1 and 2 pipe diameters gave the highest and lowest pressure recovery respectively compared to single orifice arrangement. The current study provides an insight into methods of pressure control without redesigning the complete flow system.

Keywords: Pressure drop, Multiple orifices, Computational methods, Separation zone, Reattachment zone.

1. Introduction

Many engineering applications involving piping systems utilize flow passage restrictions such as control valves and orifices to achieve control of flow rates and pressures. Accurate determination of flow characteristics through these restrictions especially orifices is important for industrial operations such as control measures in HVAC, quality control in food processing industry, metering of high viscous liquids and calibrating tools in metrology of liquid and gas flows [1]. Single orifices are also used to enhance uniformity of flow distribution and exchange of heat and mass as applicable in pre-mixed combustion [2]. When orifices are also used as flow restriction devices for the sake of pressure control, flowrate control or both, this may result in high hydraulic losses, severe erosion in the presence of solid particles; cavitation in liquid flows, choking in gas flows in addition to noise and vibration. Flow restricting orifices are used in many engineering applications such as in downstream side of a blowdown valve to ensure controlled flow rate in blowdown piping or blowdown header. They are also carefully designed and used in pump recirculation lines for the sake of preventing cavitation/pump starvation. The restricting orifice may have one-hole or multiple-holes geometry where the multiple-holes orifice is designed for achieving lower pressure drop while having high discharge coefficients [3, 4].

In some applications, the required pressure drop is too high to be achieved by a single orifice without problems such as liquid flashing, flow-choking or severe erosion resulting from high flow velocities. In such cases, a multistage restricting orifice can be used to achieve the required pressure drop through the effective arrangement of the orifices and optimum geometry design as applicable in the pipe letdown line in cooling systems of power plants and other process controls [5]. Due to the change in flow passage geometry across the orifice plate, the flow structure experience the greatest sudden change in flow turbulence parameters [6]. The complex nature of the flow through an orifice is further aggravated when passing through multiple orifices located close to each other. The aggressive nature of the flow in such combined geometries causes failures in many energy and oil & gas transportation systems due to variety of degradation mechanisms such as cavitation erosion, erosion-corrosion [7], thermal fatigue, flow-accelerated corrosion (FAC) [8]-[9], liquid droplet

impingement erosion (LDIE) [10] and internal flow fluctuations causing noise and vibration which may excite the confining surface [11]. This severely affects both safety and reliability of these systems and sometime lead to fatalities and huge economic loss [8]. All of these failure modes strongly depend on the flow characteristics downstream of the orifices and the flow instabilities generated within the complex geometry of the flow passage.

The lack of established standards for such orifice arrangements makes it difficult for the practicing engineer to predict the pressure drop, liquid flashing, flow choking and erosion characteristics. The difficulty in predicting the main flow features in multi-stage orifices arises from the strong influence of the spacing between the orifices on the flow structure prevailing in between the orifices and downstream of the last one. Therefore, the present study considers the investigation flow characteristics in a serial arrangement of two ANSI specified thin concentric bevel-edged orifices of similar sizes placed in a one-inch internal diameter horizontal pipe by computational analysis using FLUENT 12.1 CFD code.

2. Governing Equations and Computational Model

The flow field characteristics of the steady, incompressible, turbulent flow through an orifice is obtained by solving the following time-averaged continuity, momentum and turbulence equations:

$$\frac{\partial}{\partial x_j}(\rho \bar{U}_j) = 0 ; j=1, 2 \quad (1)$$

$$\frac{\partial}{\partial x_j}(\rho \bar{U}_i \bar{U}_j) + \frac{\partial}{\partial x_j}(\rho \overline{u_i u_j}) = -\frac{\partial p}{\partial x_j} + \frac{\partial}{\partial x_j} \left(\mu \frac{\partial U_i}{\partial x_j} \right) \quad (2)$$

where the static pressure is denoted p and the Reynolds stress tensor is given by

$$\rho \overline{u_i u_j} = \left[\mu_{eff} \left(\frac{\partial \bar{U}_i}{\partial x_j} + \frac{\partial \bar{U}_j}{\partial x_i} \right) \right] - \frac{2}{3} \rho k \delta_{ij} \quad (3)$$

$\mu_{eff} = \mu_t + \mu$ is the effective viscosity and δ_{ij} is Kronecker delta ($\delta_{ij} = 1$ for $i = j$ and $\delta_{ij} = 0$ for $i \neq j$) and turbulence viscosity is calculated from

$$\mu_t = \rho C_\mu \frac{k^2}{\varepsilon} \quad (4)$$

C_μ is expressed as a variable defined as $\frac{1}{A_0 + A_S \frac{k U^*}{\varepsilon}}$ where, $U^* = \sqrt{S_{ij} S_{ij} + \bar{\Omega}_{ij} \bar{\Omega}_{ij}}$

and $\bar{\Omega}_{ij} = \Omega_{ij} - 2\epsilon_{ijk} \omega_k$, $\Omega_{ij} = \bar{\Omega}_{ij} - \epsilon_{ijk} \omega_k$, $\bar{\Omega}_{ij}$ represents the mean-rate-of rotation tensor in the rotating reference frame with the angular velocity ω_k . A_0 and A_S are model constants and are expressed as $A_0 = 4.04$ and $A_0 = \sqrt{6} \cos \phi$ where $\phi = \frac{1}{3} \cos^{-1} \sqrt{6} W$, $W = \frac{S_{ij} S_{jk} S_{ki}}{\bar{\mathcal{S}}^3}$, $\bar{\mathcal{S}} = \sqrt{S_{ij} S_{ij}}$, $S_{ij} = \frac{1}{2} \left(\frac{\partial u_j}{\partial x_i} + \frac{\partial u_i}{\partial x_j} \right)$

The above equations were solved using the Realizable $k-\varepsilon$ model. It has been found that this model is more accurate than all of the $k-\varepsilon$ models especially for separated flows, boundary layer flows involving high pressure gradients and flows with complex flow structures and this makes it suitable for the current problem.

The turbulence kinetic energy (k) and turbulence kinetic energy dissipation rate are expressed as:

$$\frac{\partial}{\partial x_j}(\rho \bar{U}_j k) = \frac{\partial}{\partial x_j} \left(\frac{\mu_{eff}}{\sigma_k} \frac{\partial k}{\partial x_i} \right) + G_k - \rho \varepsilon \quad (5)$$

$$\frac{\partial}{\partial x_j}(\rho \bar{U}_j \varepsilon) = \frac{\partial}{\partial x_j} \left(\frac{\mu_{eff}}{\sigma_\varepsilon} \frac{\partial \varepsilon}{\partial x_i} \right) + \rho C_1 S \varepsilon - \rho C_2 \frac{\varepsilon^2}{k + \sqrt{\frac{\mu}{\rho} \varepsilon}} \quad (6)$$

where G_k represents the turbulence kinetic energy production due to mean velocity gradients and calculated as

$$G_k = -\rho \overline{u_i u_j} \frac{\partial \bar{U}_j}{\partial x_i} \quad (7)$$

σ_k and σ_ε are the effective Prandtl numbers for turbulence kinetic energy and its dissipation rate, respectively. C_1 is a function of k/ε as this shows that the model takes into consideration the strain rate and streamline curvature which makes it suitable for this study and it is expressed as $\left[0.43, \frac{\eta}{\eta+5}\right]$, $\eta = S \frac{k}{\varepsilon}$, where S is related to deformation strain tensor by the relation $\sqrt{2S_{ij}S_{ij}}$, with $S_{ij} = 0.5((\partial u_j/\partial x_i) - (\partial u_i/\partial x_j))$. The constants of the realizable k- ε model have specified values of $C_2 = 1.9$, $\sigma_k = 1.0$ and $\sigma_\varepsilon = 1.2$.

One of the important parameters characterizing the flow through a double-orifice arrangement is the pressure drop (Δp) which depends on fluid properties (ρ , μ), flow average velocity, U_{av} , orifice diameter ratio, D_r , pipe size, D , surface roughness, k_s , axial distance, x , and orifice spacing for double orifice arrangement, S . Mathematically, this can be expressed as

$$\Delta p = f(\rho, \mu, U_{av}, D, D_r, \varepsilon, x, S) \quad (8)$$

Based on Buckingham Π -theorem, the relationship between the above variables can be written in dimensionless form as,

$$\frac{\Delta p}{0.5\rho U_{av}^2} = f\left(\text{Re}, D_r, \frac{k_s}{D}, \frac{x}{D}, \frac{S}{D}\right) \quad (9)$$

The pipe inlet is subjected to velocity inlet boundary condition while the no-slip and non-penetration conditions are imposed at the pipe and orifice walls. The downstream boundary is assumed to have pressure outlet condition to cater for possible backflow that may occur in the flow domain shown in Figure 1. The flow velocity field is assumed axisymmetric and that limits velocity variations to radial and axial directions. The turbulence length scale and turbulence intensity (\sqrt{k}/\bar{U}) are set as internal pipe diameter and 2% respectively to specify inlet conditions for turbulent kinetic energy and dissipation rate. The values of k and ε in the flow domain are controlled by the governing equations for turbulence model.

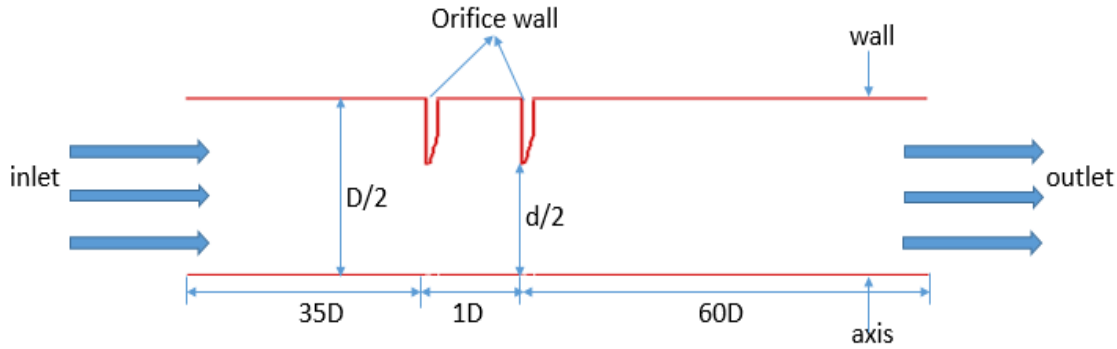


Fig. 1: Schematics of flow domain around the orifice.

The convergence criterion is set such that solution is reached when the residuals of mass continuity, velocity components, turbulence kinetic energy and dissipation rates are unchanging at values $< 10^{-6}$ and the mass-weighted average of pressure and velocity at 5 pipe diameters upstream and downstream and at the orifice face are monitored as done by Shah et al. [12]. The geometry was discretized to achieve fine grids at the walls and regions around the orifice for better prediction of wall parameters and steep change in velocity respectively. The independence of computational solution on mesh density were carried out by increasing the number of finite volumes in two steps from 6×10^4 to 1.2×10^5 and then 2.4×10^5 . A comparison of the axial variation of normalized centerline axial velocity among the grid densities for the case of inlet velocity of 2m/s and $D_r = 0.63$ (Figure 2) shows a difference less than 2%. This implies that the higher mesh densities have negligible effect on the results.

2. Results and Discussion

The orifice influences the flow field both upstream and downstream of the orifice plate. Figure 3a represents the velocity vectors for a single orifice of diameter ratio $D_r = 0.63$ at $V_i = 2\text{ m/s}$. It is evident that the fully developed velocity profile becomes distorted as the flow approaches the upstream face of the orifice plate. The flow accelerates towards the orifice throat by contraction process which extends downstream the orifice plate as the flow is driven by the vortex structures formed due to flow separation to a point of minimum area of jet flow called vena contracta. Downstream of the vena contracta the flow decelerates and continues to develop until reaching the fully developed region. The vena contracta is characterized by maximum velocity and minimum pressure as shown in Figure 3b.

Figure 4 shows the streamline patterns for flows involving orifices of $D_r = 0.63$ in a single orifice configuration for the case of $V_i = 2\text{ m/s}$. The regions of recirculation immediately downstream of the orifice plate and reattachment further downstream are clearly shown in the figure. The streamlines are drawn with constant increments of the stream function ($\Delta\psi$) in order to identify regions of low and high velocities. Accordingly, it is clear from the figure that the flow velocity increases as the flow approaches the orifice in the upstream side while decreases towards the reattachment zone in the downstream side. It is also evident that the lowest velocity occurs in the recirculation zone. The size of the recirculation zone is strongly dependent on the orifice diameter ratio and get larger as the diameter ratio decreases. Such features of the flow domain are very important for predicting erosion intensity at different locations of the pipe wall. Previous studies by Ahmed et al. [8] showed that separation of flow at the throat of an orifice produces downstream field features possessing higher velocities, streamlines with large curvatures, formation of recirculation and reattachment zones.

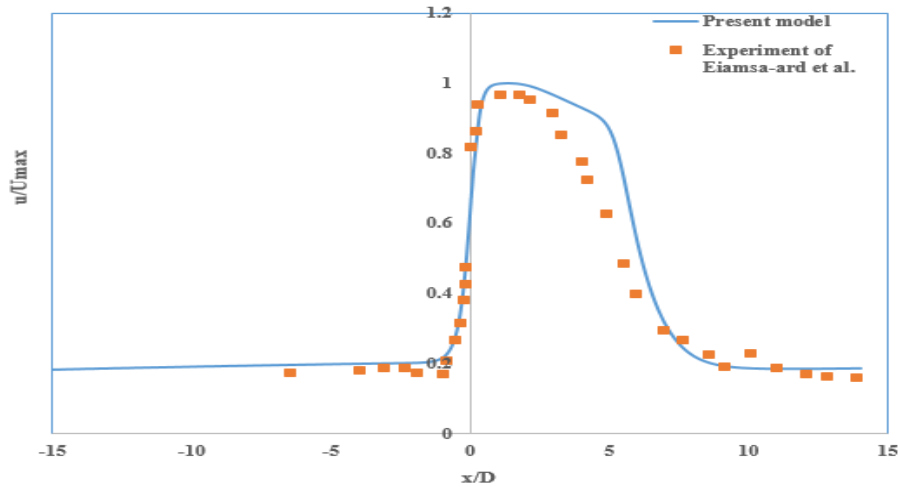


Fig. 2: Comparison between the numerical result from the present model and the experimental data of Eiamsa-ard et al. [13].

The effects of placing a second identical orifice at axial distances of 1D and 2D downstream of the first one on the velocity distribution, pressure drop and skin friction coefficient were also investigated. Figure 5 shows contour plots for the magnitude of the flow velocity upstream and downstream of the two orifices keeping in mind that the figure has been stretched in the vertical direction for better identification of the different velocity zones. The presence of vena contracta immediately downstream of the first orifice is qualitatively similar to that observed in the case of a single orifice flow (Figure 3b). It is also clear from the figure that the presence of a second orifice at 1D and 2D spacing disrupts the recirculation and reattachment zones caused by the first orifice.

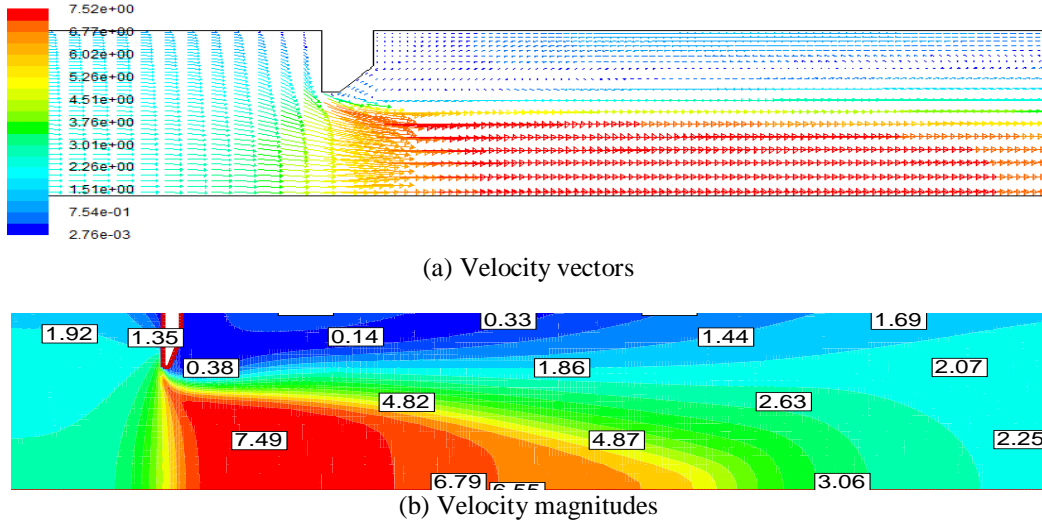


Fig. 3: Contour plots of velocity vectors and velocity magnitude (m/s) downstream orifice, for single orifice $Dr = 0.63$, $Vi = 2\text{m/s}$.

In addition, the placement of the second orifice creates a new flow region in the spacing between the two orifices characterized by a high velocity jet-like flow in the inner region (core region) surrounded by a low velocity donut-shaped vortex (recirculating flow) in the outer region (wall region) as clearly visible in the streamline plots for the same two cases shown in Figure 5. In the case of 1D spacing (Figure 5a), the recirculating flow region located in the space between the two orifices is characterized by higher velocity near the second orifice plate and lower velocity downstream of the first one. On the other hand, the streamlines in the region between the two orifices in the case of 2D spacing (Figure 5b) exhibits a longer recirculation zone occupying the entire length of orifice spacing in addition to the presence of a second low velocity recirculation zone located near the second orifice plate. The streamlines in the core region also exhibit a wider jet associated with lower axial velocities as the flow approaches the second orifice as well as the formation of a vena contracta downstream of the second orifice as shown in the same figure. This makes the flow structure upstream and downstream of the second orifice in the case of 2D spacing totally different from that in the 1D spacing (Fig.5a). The presence of this vena contracta downstream of the second orifice led to the formation of a recirculation zone possessing higher velocity and higher vorticity in comparison with that in the case of 1D spacing (Figure 5a). Consequently, the flow structure upstream of the second orifice in both cases of 1D and 2D spacing is completely different from that upstream of the orifice in the single orifice configuration. The jet-like flow approaching the second orifice (Figures 5a, b) has a significant impact on the flow structure downstream of the second orifice, thus affecting the velocity distribution, separation and reattachment flow zones as well as the vortex formation and the recirculating flow zone.

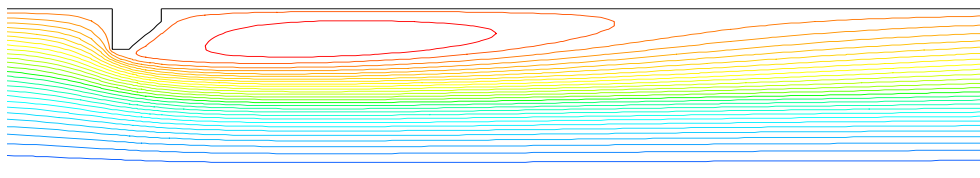
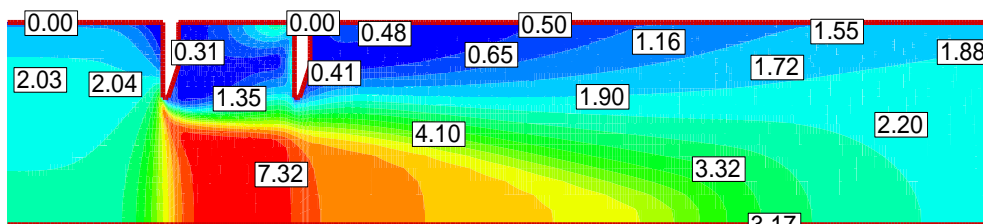
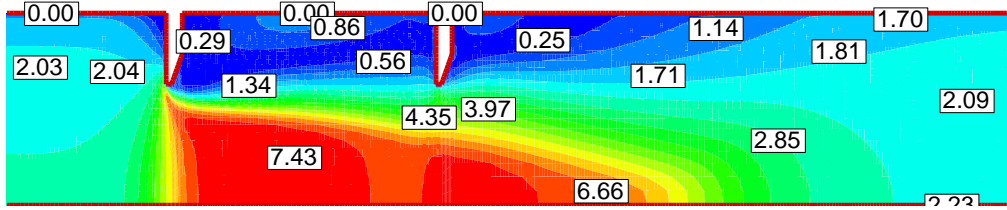


Fig. 4: Comparison between streamline plots for a single orifice at $Vi = 2\text{m/s}$, $Dr = 0.63$.



a) Double orifice-1D-spacing



b) Double orifice-2D-spacing

Fig. 5: Contours plot of velocity magnitude (m/s) in a double-orifice arrangement with $D_r = 0.63$, $V_i = 2\text{m/s}$ for the cases of a) 1D spacing, and b) 2D spacing.

Figure 6 shows a comparison between the normalized centerline velocity for the three arrangements of single orifice, double orifices with 1D and 2D spacing for $D_r = 0.63$ and $V_i = 2\text{ m/s}$. It can be seen that the peak velocity downstream of a single orifice and the first orifice of double-orifice arrangement exists in the same location but with slightly higher velocity in double-orifice cases. Moreover, the axial velocity variation for double orifice with 1D spacing shows a trend of negative slope similar in magnitude to that of single orifice flow up to $x \approx 4D$. This slope extends further by approximately $x = 0.5D$ beyond that of single orifice (i.e. up to $x \approx 4.5D$) before it changes to a steep negative slope. This is attributed to the presence of the second orifice that helped to maintain the jet-like flow over longer distance thereby delaying the sharp drop in velocity signifying the approach of the reattachment zone. In the case of double orifice flow with 2D spacing, a second peak occurs downstream the second orifice (at approximately $x \approx 2.5D$) due to the presence of vena contracta. A comparison between the axial velocity in the immediate region downstream the second orifice in double orifices configuration and that of single orifice shows that the double orifice with 2D spacing has the highest velocity.

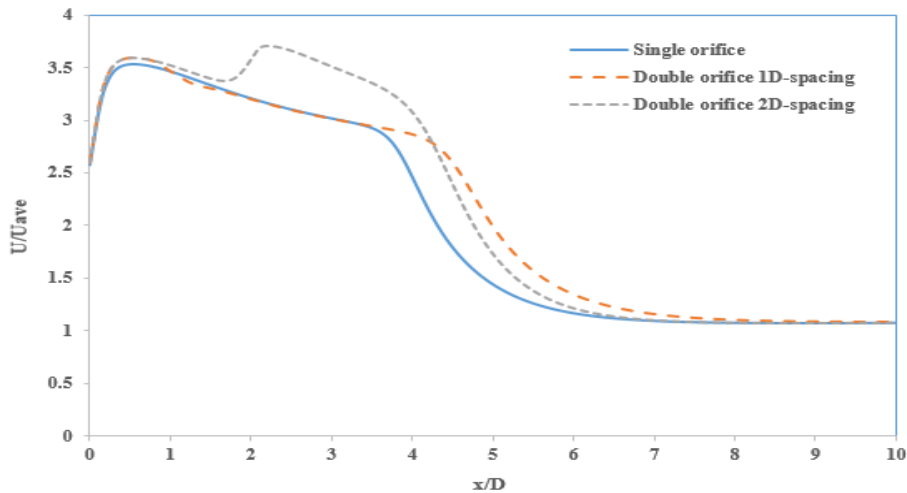


Fig. 6: Comparison of centerline axial velocity for different configurations of single orifice, double orifice with 1D and 2D spacing for $D_r = 0.63$ and $V_i = 2\text{m/s}$.

Another important property characterizing flow through a restricting orifice is the pressure drop resulting from hydraulic losses between far upstream and far downstream of the orifice (or double-orifice arrangement) as a result of the presence of such flow-passage restriction. As presented in Eq. (9), the pressure coefficient $(\Delta p / 0.5 \rho U_{av}^2)$ depends on Re , D_r , k_s / D and S / D . A typical static pressure variation has a linear portion in far upstream and far downstream zones, both of equal negative gradients in the downstream section as shown graphically in Figure 7. The pressure drop caused by the orifice results largely from the abrupt change in the flow passage cross-sectional area causing high level of turbulence and thus creating considerable hydraulic losses. This pressure drop can be obtained from the computed (or measured) static pressure variation by extrapolating the far upstream and far downstream linear pressure variations towards the orifice plate as shown in the figure. The effects of inlet flow velocity ($V_i = 1\text{ m/s}$, 2 m/s , 4 m/s) and orifice geometry ($D_r = 0.5$, 0.63 ,

and 0.77) on the pressure drop in the three different configurations of single orifice and double orifice with 1D and 2D spacing are considered in some detail. The value of Δp given in Eq. (8) represents the difference in pressure between any given location and a reference pressure. The selection of the reference pressure differs from one study to another. For example, Ahmed et al. [8] chose the outflow pressure (p_{out}) as the reference pressure while Manmatha & Sukanta [2] chose the pressure at an axial distance of 5-orifice diameters upstream the orifice plate. In this study, the reference pressure adopted is the static pressure (P_{5D}) at axial distance of 5D upstream the orifice plate (i.e. at $x = -5D$) with the origin located at the orifice plate.

The other interesting phenomenon is found when comparing the values of the pressure drop, Δp , between far upstream and far downstream ($x = -5D$ and $x = 8D$) of the orifice plate for the two cases of double orifice with 1D spacing and $D_r = 0.63$ (Figure 17a) and a single orifice having the same diameter ratio (Figure 7) considering the same inlet velocity, $V_i = 2$ m/s. The obtained pressure drop in the case of double orifice with 1D spacing was 12 kPa while reaching 15 kPa in the case of a single orifice. In this case, the indicated pressure drop is also a measure of the total hydraulic losses. This means that a double-orifice arrangement (1D spacing) results in total hydraulic losses about 20% less than that of a single orifice even though the first one has two constrictions while the second one has only one constriction. The same phenomenon prevails in the case of $D_r = 0.5$ where the pressure drop is 40 kPa in the case of double-orifice (1D spacing) while reaching 52 kPa in the case of a single orifice. This indicates that the hydraulic losses in this double orifice arrangement are 23% less than that of a single orifice. The case of $D_r = 0.77$ did not show a contrary result where the double orifice 1D-spacing gave a 12.5% reduction in pressure drop relative to the single orifice configuration. In order to verify the existence of this phenomenon, pressure measurements with simple manometers were taken for the two arrangements with $D_r = 0.63$ but for a velocity of 0.555 m/s (corresponding to $Re = 1.4 \times 10^4$). Figure 8 shows the pressure variation for the two cases of a single orifice and a double orifice with 1D spacing. This figure clearly indicates the presence of the above phenomenon and also validates the accuracy of the computational model.

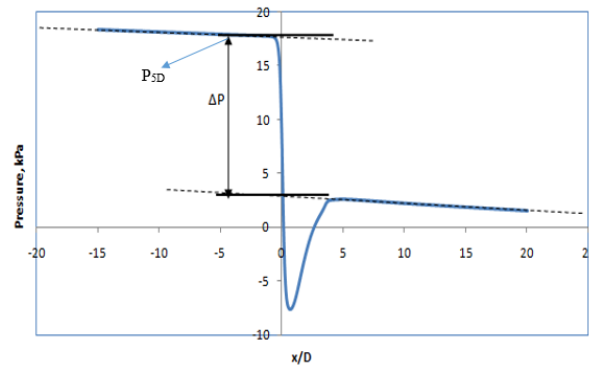


Fig. 7: Illustration of determination of ΔP from static pressure values.

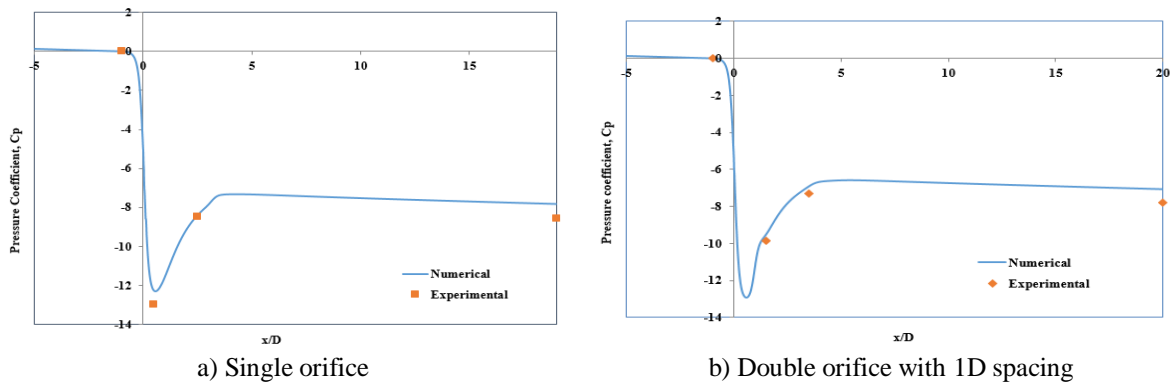


Fig. 8: Comparison between computational and experimental pressure variation for the case of $D_r = 0.63$, $V_i = 0.555$ m/s.

Figure 9 indicates insignificant effect of Re on the variation of the pressure coefficient, C_p , from the upstream boundary up to the vena contracta where the minimum pressure is attained in the case of 1D spacing. Downstream of the vena contracta, the effect of Re is small and characterized by slightly higher pressure recovery at higher velocities. The second local minimum pressure occurs at the second vena contracta and characterized by a pressure higher than that occurring at the first vena contracta. The value of C_p far downstream is almost the same for all velocities however, the pressure drop in the case of 2D spacing is much higher than that for the 1D spacing as can be seen in Figure 9.

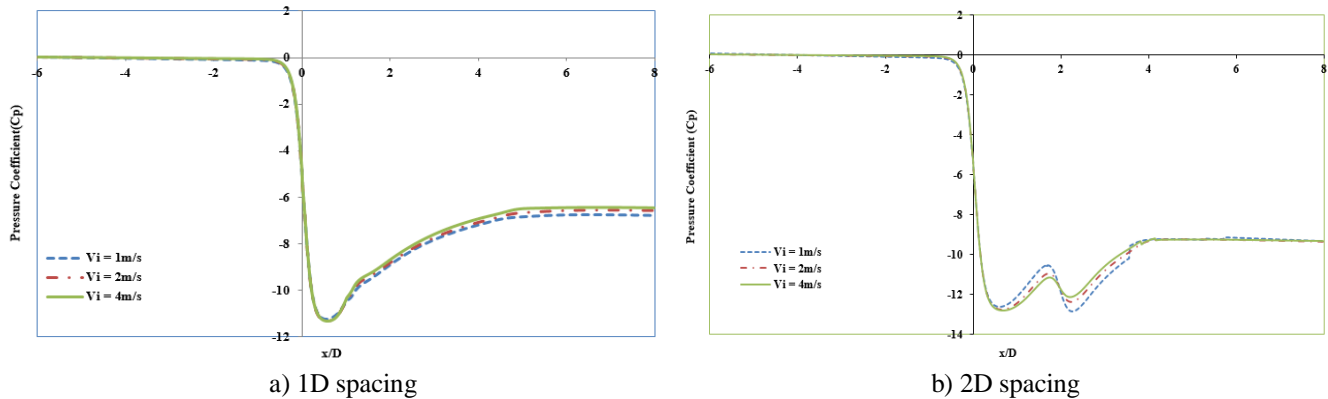


Fig. 9: Effect of inlet velocity on the pressure variation for a double-orifice with $D_r = 0.63$.

4. Conclusion

The flow field characteristics in multi-stage orifice system have been numerically investigated by considering the effects of flow inlet velocity, orifice geometry, orifice spacing on velocity and pressure distribution. The inlet flow velocities considered are 1m/s, 2m/s, and 4m/s, orifice spacing of one and two pipe diameters, orifice diameter ratios of 0.63. The flow characteristics downstream of the multiple orifice arrangement is qualitatively similar to that downstream a single orifice of the same size in terms of the existence recirculation zone, reattachment zone and shear layer region. Some important differences in the flow structure are identified upstream of the second orifice in the double-orifice configurations which has a jet-like flow in the core region surrounded by donut-shaped vortical flow in the wall region influencing the downstream velocity field and pressure recovery region. The double orifice arrangements produce a peak velocity that is slightly higher than single orifice with corresponding orifice size but at a similar location. On the other hand, the double orifice with two pipe diameter spacing produces a second peak velocity downstream the second orifice. The pressure distribution profiles across the three configurations are similar but the least and highest pressure drop were recorded in the double orifice configurations with one and two pipe diameter spacing respectively.

Acknowledgements

The authors wish to acknowledge the support received from King Fahd University of Petroleum & Minerals, Dhahran, Saudi Arabia and the Natural Sciences and Engineering Research Council of Canada (NSERC) during the course of this study.

References

- [1] T. Gronych, M. Jeřáb, L. Peksa, J. Wild, F. Staněk, and M. Vičar, "Experimental study of gas flow through a multi-opening orifice," *Vacuum*, vol. 86, no. 11, pp. 1759-1763, May 2012.
- [2] M. K. Roul and S. K. Dash, "Single-Phase and Two-Phase Flow Through Thin and Thick Orifices in Horizontal Pipes," *J. Fluids Eng.*, vol. 134, no. 9, p. 91301, 2012.
- [3] V. K. Singh and T. John Tharakan, "Numerical simulations for multi-hole orifice flow meter," *Flow Meas. Instrum.*, vol. 45, pp. 375-383, 2015.
- [4] C. Alimonti, G. Falcone, and O. Bello, "Two-phase flow characteristics in multiple orifice valves," *Exp. Therm. Fluid Sci.*, vol. 34, no. 8, pp. 1324-1333, 2010.

- [5] W. Haimin, X. Shujuan, S. Qingyi, Z. Caimin, L. Hao, and C. Eryun, "Experiment study on pressure drop of a multistage letdown orifice tube," *Nucl. Eng. Des.*, vol. 265, pp. 633-638, 2013.
- [6] H. P. Rani, T. Divya, R. R. Sahaya, V. Kain, and D. K. Barua, "Numerical investigation of energy and Reynolds stress distribution for a turbulent flow in an orifice," *Eng. Fail. Anal.*, vol. 34, pp. 451-463, 2013.
- [7] M. A. Nemitallah, R. Ben-Mansour, M. A. Habib, W. H. Ahmed, I. H. Toor, Z. M. Gasem, and H. M. Badr, "Solid Particle Erosion Downstream of an Orifice," *J. Fluids Eng.*, vol. 137, no. 2, pp. 021302, 2014.
- [8] W. H. Ahmed, M. M. Bello, M. El Nakla, and A. Al Sarkhi, "Flow and mass transfer downstream of an orifice under flow accelerated corrosion conditions," *Nucl. Eng. Des.*, vol. 252, pp. 52-67, 2012.
- [9] J. Xiong, X. Cheng, and Y. Yang, "Numerical investigation on mass transfer enhancement downstream of an orifice," *Int. J. Heat Mass Transf.*, vol. 68, pp. 366-374, 2014.
- [10] K. M. Hwang, C. K. Lee, and C. R. Choi, "A Study on the Cause Analysis for the Wall Thinning and Leakage in Small Bore Piping Downstream of Orifice," *World J. Nucl. Sci. Technol.*, vol. 4, no. 1, pp. 1-6, 2014.
- [11] M. K. Bull and N. G. Agarwal, "Characteristics of flow separation due to an orifice plate in fully-developed turbulent flow-pipe," 1983.
- [12] M. S. Shah, J. B. Joshi, A. S. Kalsi, C. S. R. Prasad, and D. S. Shukla, "Analysis of flow through an orifice meter: CFD simulation," *Chem. Eng. Sci.*, vol. 71, pp. 300-309, 2012.
- [13] S. Shaaban, "Optimization of orifice meter's energy consumption," *Chem. Eng. Res. Des.*, vol. 92, no. 6, pp. 1005-1015, 2014.